Product Datasheet

Histone H2AX [p Ser139] Antibody
NB100-2280

Unit Size: 0.1 ml

Store at 4C. Do not freeze.

www.novusbio.com technical@novusbio.com

Reviews: 1 Publications: 54

Protocols, Publications, Related Products, Reviews, Research Tools and Images at:
www.novusbio.com/NB100-2280

Updated 2/17/2025 v.20.1

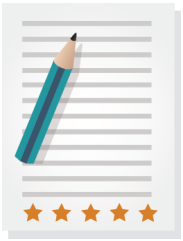

NB100-2280

Histone H2AX [p Ser139] Antibody

Product Information	
Unit Size	0.1 ml
Concentration	0.1 mg/ml
Storage	Store at 4C. Do not freeze.
Clonality	Polyclonal
Preservative	0.09% Sodium Azide
Isotype	IgG
Purity	Immunogen affinity purified
Buffer	TBS and 0.1% BSA
Target Molecular Weight	15 kDa

Product Description	
Host	Rabbit
Gene ID	3014
Gene Symbol	H2AX
Species	Human, Mouse, Canine
Reactivity Notes	Based on sequence percent identity: Gorilla (100%), Macaque (100%), Canine reactivity reported in scientific literature (PMID: 26991424).
Marker	DNA Double-strand break marker
Immunogen	This Histone H2AX [p Ser139] Antibody was developed against a synthetic phospho-peptide, which represented a portion of the C-terminus of human histone H2AX surrounding phosphorylated serine 139 (GeneID 3014).
Notes	Licensed to Novus Biologicals LLC under U.S. Patent Nos. 6,362,317 and 6,884,873.

Product Application Details	
Applications	Western Blot, Simple Western, Immunocytochemistry/ Immunofluorescence, Immunohistochemistry, Immunohistochemistry-Frozen, Immunohistochemistry-Paraffin
Recommended Dilutions	Western Blot 1:100-1:2000, Simple Western 1:20, Immunohistochemistry, Immunocytochemistry/ Immunofluorescence 1:100 - 1:500, Immunohistochemistry-Paraffin 1:100-1:500, Immunohistochemistry-Frozen
Application Notes	Epitope exposure is recommended. Epitope exposure with citrate buffer will enhance staining. Likely to work with frozen sections. Use in WB reported in scientific literature (PMID 24415760). Use in IHC-Frozen reported in scientific literature (PMID 26577699). In Simple Western only 10 - 15 uL of the recommended dilution is used per data point. See Simple Western Antibody Database for Simple Western validation: Tested in Jurkat lysate, separated by Size, antibody dilution of 1:20, apparent MW was 30 kDa. Separated by Size-Wes, Sally Sue/Peggy Sue.

Images

Immunohistochemistry: Histone H2AX [p Ser139] Antibody [NB100-2280] - Biological and molecular analysis of cutaneous wound healing in p73+/+ and p73-/- mice. Representative micrographs of immunohistochemistry (IHC) staining for Histone H2AX [p Ser139] in skin specimens from p73+/+ and p73-/- mice 10 days after wounding. All scale bars represent 50 um. Regions of the skin are labeled as: IFE, HF, epidermal wound edge (WE), and newly-formed epidermis of the wound (W); and the dotted line indicates the border between the WE and W. *p-value < 0.05, **p-value < 0.01, ***p-value < 0.001. Image collected and cropped by CiteAb from the following publication (https://dx.plos.org/10.1371/journal.pone.0218458), licensed under a CC-BY license.

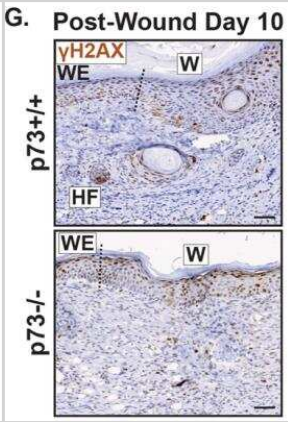

Simple Western: Histone H2AX [p Ser139] Antibody [NB100-2280] - Simple Western lane view shows a specific band for Histone H2AX [p Ser139] in 0.2 mg/ml of Jurkat lysate(s). This experiment was performed under reducing conditions using the 12 - 230 kDa separation system.

Immunohistochemistry: Histone H2AX [p Ser139] Antibody [NB100-2280] - Telomere dysfunctional induced foci (TIF) in HBV-related multistep hepatocarcinogenesis and the correlations thereof with stathmin and elongation factor 1alpha (EF1alpha) expression. A. Representative features of colocalization of Histone H2AX [p Ser139] and telomeric DNA in defined lesions of human multistep hepatocarcinogenesis. TIF are indicated by colored arrowheads: blue, DAPI; green, gamma H2AX; red, telomeres; yellow, TIF. Image collected and cropped by CiteAb from the following publication (https://translational-medicine.biomedcentral.com/articles/10.1186/1479-5876-12-154) licensed under a CC-BY license.

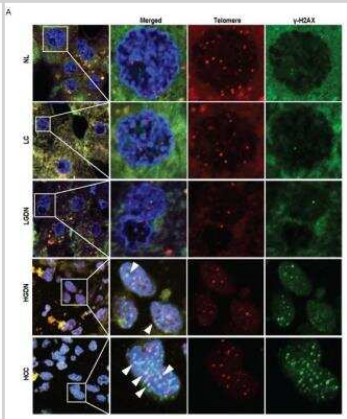

Immunohistochemistry-Paraffin: Histone H2AX [p Ser139] Antibody [NB100-2280] - Detection of human Histone H2AX [p Ser139] antibody by immunohistochemistry. Sample: FFPE section of human seminoma. Antibodies: Affinity purified rabbit Histone H2AX [p Ser139] antibody used at a dilution of 1:500. Detection: DAB.

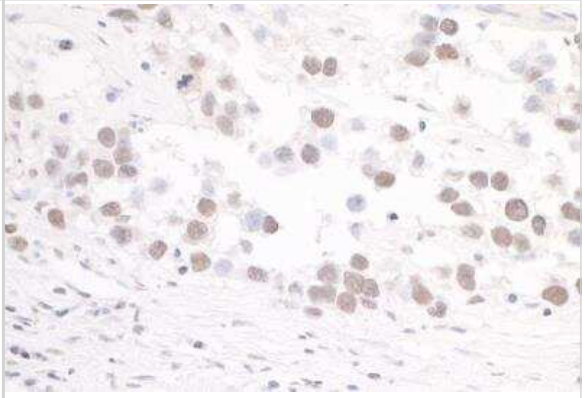

Immunohistochemistry: Histone H2AX [p Ser139] Antibody [NB100-2280] - Detection of Mouse Histone H2AX [p Ser139] by Immunohistochemistry. Sample: FFPE section of mouse colon carcinoma CT26. Antibodies: Affinity purified rabbit Histone H2AX [p Ser139] antibody. Detection: DAB.

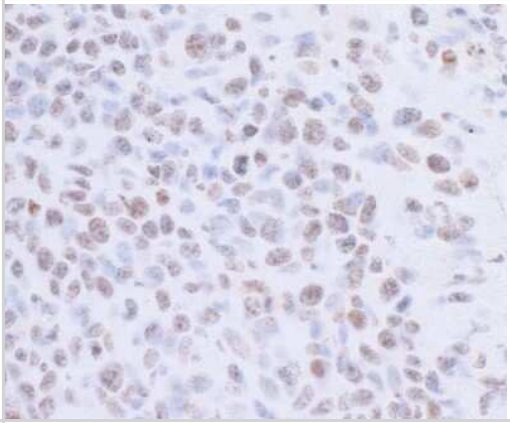

Simple Western: Histone H2AX [p Ser139] Antibody [NB100-2280] - Electropherogram image(s) of corresponding Simple Western lane view. Histone H2AX [p Ser139] antibody was used at 1:20 dilution on Jurkat lysate(s).

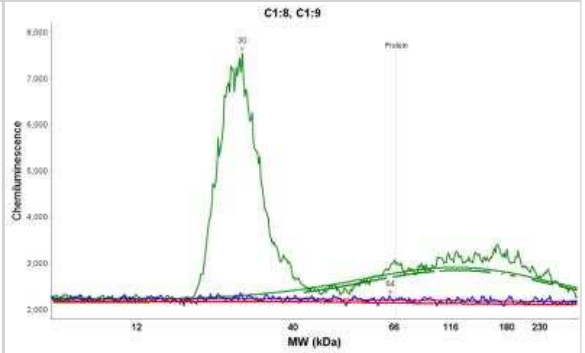

Immunocytochemistry/ Immunofluorescence: Histone H2AX [p Ser139] Antibody [NB100-2280] - Treatment with anti-thyroid drug protected RPE & photoreceptors from oxidative damage induced by NaIO3.RPE & retinal oxidative damage were evaluated by immunofluorescence labeling of p-γH2AX & 8-OHdG on the RPE whole mounts & retinal sections at 3 days post-NaIO3 injection. a Shown are representative images of p-γH2AX immunofluorescence labeling on the RPE whole mounts. b Shown are representative images of p-γH2AX & 8-OHdG immunofluorescence labeling on the retinal sections, & corresponding quantitative analysis for p-γH2AX labeling. ONL, outer nuclear layer; INL, inner nuclear layer. Data represented the mean ± SEM for 5 mice per group (*p < 0.05). Image collected & cropped by CiteAb from the following publication (https://pubmed.ncbi.nlm.nih.gov/31932580), licensed under a CC-BY license. Not internally tested by Novus Biologicals.

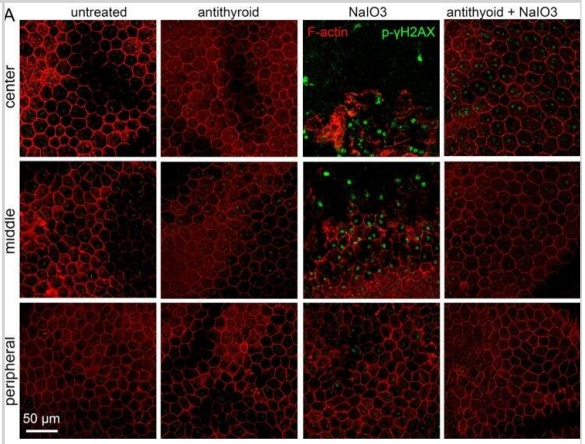

Immunocytochemistry/ Immunofluorescence: Histone H2AX [p Ser139] Antibody [NB100-2280] - Treatment with anti-thyroid drug protected RPE & photoreceptors from oxidative damage induced by NaIO3.RPE & retinal oxidative damage were evaluated by immunofluorescence labeling of p-γH2AX & 8-OHdG on the RPE whole mounts & retinal sections at 3 days post-NaIO3 injection. a Shown are representative images of p-γH2AX immunofluorescence labeling on the RPE whole mounts. b Shown are representative images of p-γH2AX & 8-OHdG immunofluorescence labeling on the retinal sections, & corresponding quantitative analysis for p-γH2AX labeling. ONL, outer nuclear layer; INL, inner nuclear layer. Data represented the mean ± SEM for 5 mice per group (*p < 0.05). Image collected & cropped by CiteAb from the following publication (https://pubmed.ncbi.nlm.nih.gov/31932580), licensed under a CC-BY license. Not internally tested by Novus Biologicals.

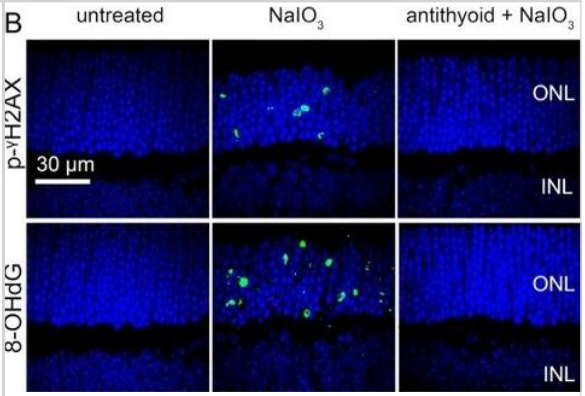

Immunocytochemistry/ Immunofluorescence: Histone H2AX [p Ser139] Antibody [NB100-2280] - RES rescued DXR-induced apoptosis through DNA-damage-P63-Caspase3 pathway in mouse oocytes. (A) Representative immunofluorescence images showing the expression of γ-H2AX in mouse oocytes. Green, γ-H2AX, Blue, DNA, Bar = 20 μm. (B) The relative immunofluorescence intensity of γ-H2AX was measured in control, DXR-treated & RES-supplemented oocytes. Experiments were repeated at least 3 times with more than 30 oocytes examined for each group. Data were presented as means ± S.E.M of three independent experiments. **means P < 0.01, *** means P < 0.001. (C) Protein levels of γ-H2AX, P63 & Active-Caspase3 were examined by Western blotting in control, DXR-treated & RES-supplemented oocytes. GAPDH was used as a loading control. The clean backgrounds for the active-Caspase-3, γ-H2AX & GAPDH is due to the exposure. Image collected & cropped by CiteAb from the following publication (https://pubmed.ncbi.nlm.nih.gov/32352929), licensed under a CC-BY license. Not internally tested by Novus Biologicals.

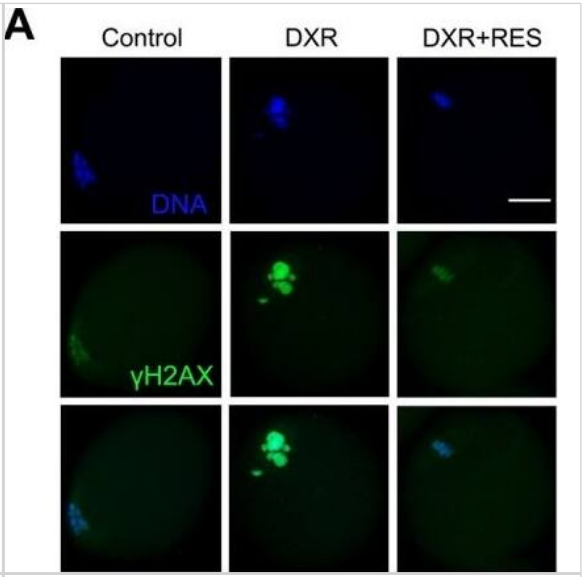

Immunohistochemistry: Histone H2AX [p Ser139] Antibody [NB100-2280] - Hepatic activation of FOXO3 induces oxidative damage & Akt activation. a Expression of Bcl2l11 (Bim), Sesn2 & Sesn3 by qPCR in livers from 9-week-old control & FOXO3CAHep transgenic mice (n = 4). b Representative IHC staining for 8-OHdG (bar = 100 μm) & quantification of 8-OHdG-positive cells as a percentage of total hepatocyte cells in livers of patients in area of small cells (SC) & large cells (LC). c Representative IHC staining for phospho-γH2AX (bar = 100 μm) & quantification of phospho-γH2AX-positive cells as a percentage of total hepatocyte cells in livers of patients in area of small cells & large cells. d Expression of Msh2 by qPCR (upper panel), Western blot analysis for MSH2 (middle panel) & densitometric quantification (lower panel) in livers from 9-week-old control & FOXO3CAHep transgenic mice (n = 4). e Western blot analysis in livers from 9-week-old control & FOXO3CAHep mice for serine-473 phospho-Akt, with Akt & GAPDH as loading control (left panel), as well as densitometric quantification (right panel). f Representative IHC staining for phospho-Akt in livers from 9-week-old control & FOXO3CAHep mice (bar = 100 μm). g Western blot analysis in livers from 9-week-old control & FOXO3CAHep mice for Rictor & GAPDH as loading control (left panel), as well as densitometric quantification (right panel) Image collected & cropped by CiteAb from the following publication (https://pubmed.ncbi.nlm.nih.gov/31488102), licensed under a CC-BY license. Not internally tested by Novus Biologicals.

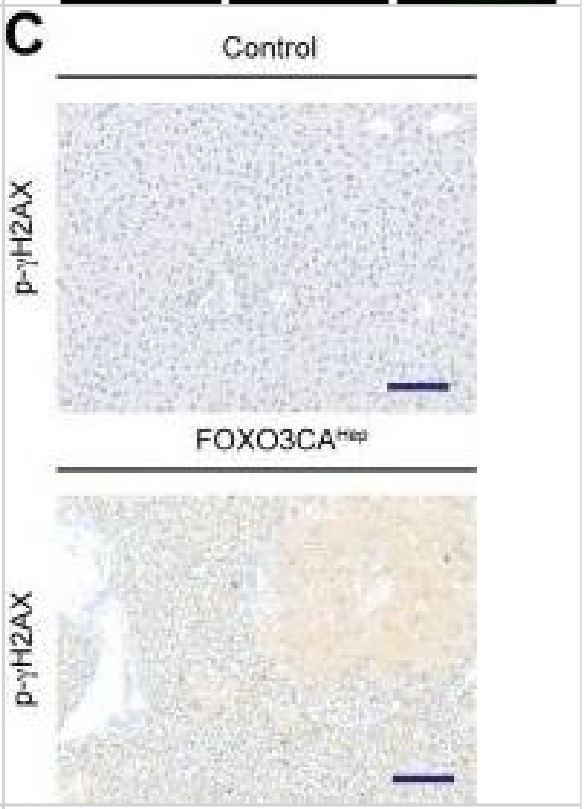

Western Blot: Histone H2AX [p Ser139] Antibody [NB100-2280] - RES rescued DXR-induced apoptosis through DNA-damage-P63-Caspase3 pathway in mouse oocytes. (A) Representative immunofluorescence images showing the expression of γ-H2AX in mouse oocytes. Green, γ-H2AX, Blue, DNA, Bar = 20 μm. (B) The relative immunofluorescence intensity of γ-H2AX was measured in control, DXR-treated & RES-supplemented oocytes. Experiments were repeated at least 3 times with more than 30 oocytes examined for each group. Data were presented as means ± S.E.M of three independent experiments. **means P < 0.01, *** means P < 0.001. (C) Protein levels of γ-H2AX, P63 & Active-Caspase3 were examined by Western blotting in control, DXR-treated & RES-supplemented oocytes. GAPDH was used as a loading control. The clean backgrounds for the active-Caspase-3, γ-H2AX & GAPDH is due to the exposure. Image collected & cropped by CiteAb from the following publication (https://pubmed.ncbi.nlm.nih.gov/32352929), licensed under a CC-BY license. Not internally tested by Novus Biologicals.

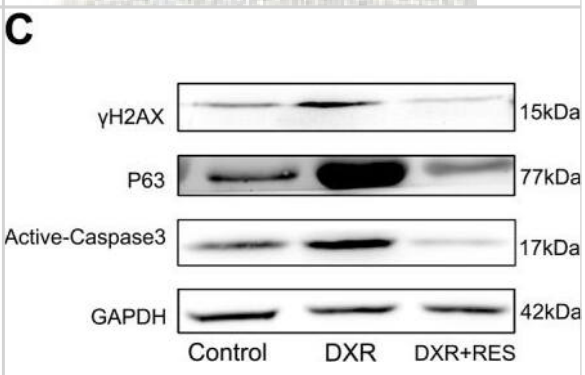

Immunocytochemistry/ Immunofluorescence: Histone H2AX [p Ser139] Antibody [NB100-2280] - Oocyte-specific deletion of Gsk-3β disrupted early folliculogenesis in mice. aGsk-3β efficiently & specifically deleted in the oocytes in cKO mouse ovary. Immunofluorescence staining for GSK-3β (green) & DDX4 (red) on 1 dpp ovary. The nucleus stained by Hoechst (blue). b Control & cKO ovaries at the indicated developmental stages. Oocytes stained w/ DDX4 (green). The nucleus stained by Hoechst (blue). c Statistical analysis showed that the total number of primordial follicle decreased significantly in 7 dpp cKO ovaries (Additional file 8: Individual data values). d Apoptotic cells increased in 1 dpp cKO ovaries compared w/ the control ovaries. TUNEL signals (green) marked apoptotic cells. The nucleus stained by Hoechst (blue). e DSBs persisted in the oocytes of 1 dpp cKO ovaries. The sections stained w/ γ-H2AX (green) & DDX4 (red). The nucleus stained by Hoechst (blue). f Ectopic RAD51 expression in the oocytes of 1 dpp cKO ovaries. The sections stained w/ RAD51 (green) & DDX4 (red). The nucleus stained by Hoechst (blue). g, h β-catenin accumulated in the cytoplasm & translocated into nucleus of the oocytes in cKO mice. g The sections stained w/ β-catenin (green) & DDX4 (red). The nucleus stained by Hoechst (blue). Arrowheads indicated oocytes showing nuclear β-catenin accumulation. h The statistic analysis demonstrated that the percentage of oocytes showing β-catenin accumulation per section increased significantly in cKO mice (Additional file 8: Individual data values). The data are presented as mean ± s.d. The asterisk (*) denotes a statistically significant difference between the control & treatment groups. *P < 0.05, **P < 0.01, & ***P < 0.001 (t test). Scale bars, 200 μm Image collected & cropped by CiteAb from the following publication (https://pubmed.ncbi.nlm.nih.gov/30866939), licensed under a CC-BY license. Not internally tested by Novus Biologicals.

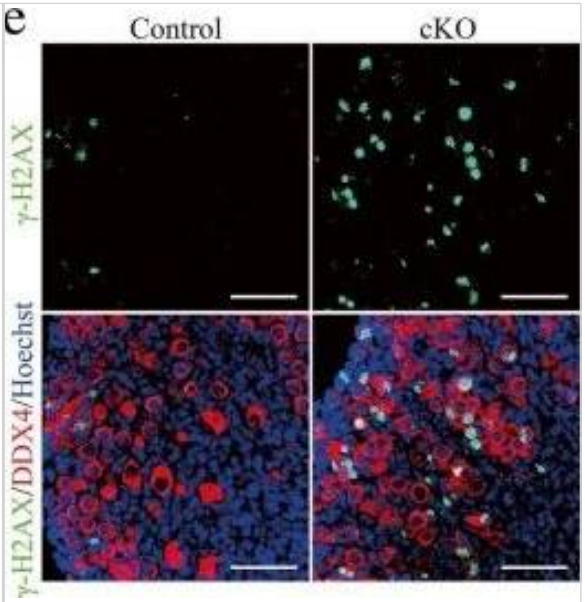

Immunohistochemistry: Histone H2AX [p Ser139] Antibody [NB100-2280] - IDO1 inhibitor enhances the efficacy of radiotherapy in vivo. 1 × 105 of SiHa tumorsphere cells were subcutaneously injected to nude mice for tumor growth. After the tumor volume reached 50 mm3, the mice were divided into four groups of non-treated (Ctrl), INCB-024360 treated (INCB), radiotherapy (Rx), or INCB-024360 plus radiotherapy (INCB + Rx). For the INCB or INCB + Rx group, mice were injected once with 50 mg/kg INCB-024360 intraperitoneally before radiotherapy. For the Rx or INCB + Rx group, mice received 2 Gy radiation per day for total 10 Gy. Mice were sacrificed at day 30 after the last radiation treatment & the xenografted tumors were taken out for picturing (A) & weighting (B). The expression of Ki-67 or p-γH2AXser139 was determined by paraffin section followed by immunohistochemical staining (C). The inserted bars indicated 50 μM. The quantification results were performed by TissueFAX software (D). * p < 0.05; ** p < 0.01. The experiments were repeated two times & data from one experiment were presented. Image collected & cropped by CiteAb from the following publication (https://pubmed.ncbi.nlm.nih.gov/32545442), licensed under a CC-BY license. Not internally tested by Novus Biologicals.

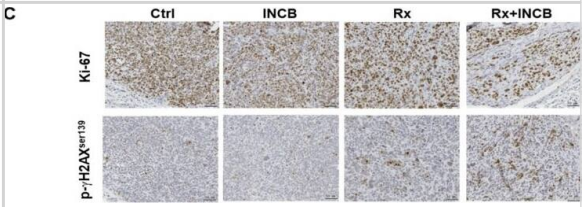

Immunocytochemistry/ Immunofluorescence: Histone H2AX [p Ser139] Antibody [NB100-2280] - Premature upregulation of TAp63 in GSK-3β-inhibited ovary. a Expression pattern of γ-H2AX in fetal & neonatal mouse ovary in vivo. Mouse ovaries from 13.5 dpc, 15.5 dpc, 17.5 dpc, & 1 dpp immunostained for γ-H2AX (green) & DDX4 (red). Nucleus stained by Hoechst (blue). γ-H2AX displayed intensive expression in germ cell nucleus from 15.5 to 17.5 dpc. b Expression pattern of TAp63 in fetal & neonatal mouse ovary in vivo. Mouse ovaries from 13.5 dpc, 15.5 dpc, 17.5 dpc, 18.5 dpc, & 1 dpp immunostained for TAp63 (green) & DDX4 (red). Nucleus stained by Hoechst (blue). TAp63 protein located w/in somatic cells in fetal ovary & began to express in germ cell nucleus from 18.5 dpc afterward. c–e TAp63 expression upregulated in fetal ovary & displayed premature localization w/in oocyte nucleus following GSK-3β inhibition. Before examination, ovaries of 14.5 dpc cultured in vitro w/ DMSO or BIO for 3 days. c qRT-PCR analysis of TAp63 mRNA level following GSK-3β inhibition (normalized to β-actin) (Additional file 8: Individual data values). d WB analysis of TAp63 protein level following GSK-3β inhibition. GAPDH used as internal control. e Immunofluorescence staining for TAp63 (green) & DDX4 (red). The nucleus stained by Hoechst (blue). TAp63 showed premature expression w/in oocyte nucleus following GSK-3β inhibition (arrowhead). f qRT-PCR results showed that relative mRNA expression level of p21, Bad, & Noxa increased significantly in GSK-3β-inhibiting ovaries (Additional file 8: Individual data values). data are presented as mean ± s.d. The asterisk (*) denotes a statistically significant difference between the control & treatment groups. *P < 0.05, **P < 0.01, & ***P < 0.001 (t test). Scale bars, 200 μm Image collected & cropped by CiteAb from the following publication (https://pubmed.ncbi.nlm.nih.gov/30866939), licensed under a CC-BY license. Not internally tested by Novus Biologicals.

a

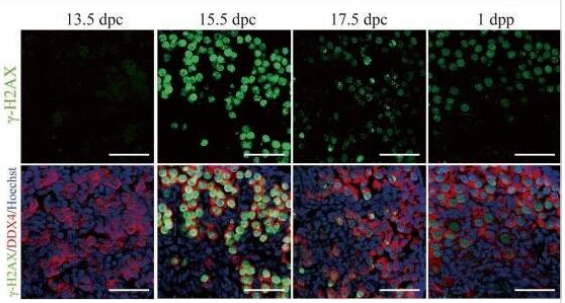

Publications

Brackman LC, Jung MS, Green EH et Al. IL-17 signaling protects against Helicobacter pylori-induced gastric cancer Gut Microbes 2024-11-26 [PMID: 39588838]

Izadifar Z, Charrez B, Almeida M et Al. Organ chips with integrated multifunctional sensors enable continuous metabolic monitoring at controlled oxygen levels Biosens Bioelectron 2024-09-05 [PMID: 39213819]

Pissas G, Tziastoudi M, Divani M et Al. Malate dehydrogenase-2 inhibition shields renal tubular epithelial cells from anoxia-reoxygenation injury by reducing reactive oxygen species J Biochem Mol Toxicol 2024-09-17 [PMID: 39287333]

McNamara KM, Sierra JC, Latour YL et Al. Spermine oxidase promotes Helicobacter pylori-mediated gastric carcinogenesis through acrolein production Oncogene 2024-11-10 [PMID: 39523394]

Sperry MM, Charrez B, Fotowat H et Al. Identification of pharmacological inducers of a reversible hypometabolic state for whole organ preservation Elife 2024-09-24 [PMID: 39316042]

Rauch H, Kitzberger C, Janghu K et al. Combining [177 Lu]Lu-DOTA-TOC PRRT with PARP inhibitors to enhance treatment efficacy in small cell lung cancer European Journal of Nuclear Medicine and Molecular Imaging 2024-07-18 [PMID: 39023784]

Boege Yannick, Malehmir Mohsen, Healy Marc E et al. A Dual Role of Caspase-8 in Triggering and Sensing ProlifeRation-Associated DNA Damage, a Key Determinant of Liver Cancer Development. Cancer Cell 2017-01-01 [PMID: 28898696]

Emily A. Bates, James A. Davies, Jana Váňová, Davor Nestić, Valerie S. Meniel, Sarah Koushyar, Tabitha G. Cunliffe, Rosie M. Mundy, Elise Moses, Hanni K. Uusi-Kerttula, Alexander T. Baker, David K. Cole, Dragomira Majhen, Pierre J. Rizkallah, Toby Phesse, John D. Chester, Alan L. Parker Development of a low-seroprevalence, αvβ6 integrin-selective virotherapy based on human adenovirus type 10 Molecular Therapy Oncolytics 2022-03-16 [PMID: 35399606]

A Deczkowska, E David, P Ramadori, D Pfister, M Safran, B At The, A Giladi, DA Jaitin, O Barboy, M Cohen, I Yofe, C Gur, S Shlomi-Lou, S Henri, Y Suhail, M Qiu, S Kam, H Hermon, E Lahat, G Ben Yakov, O Cohen-Ezra, Y Davidov, M Likhter, D Goitein, S Roth, A Weber, B Malissen, A Weiner, Z Ben-Ari, M Heikenwäld, E Elinav, I Amit XCR1+ type 1 conventional dendritic cells drive liver pathology in non-alcoholic steatohepatitis Nature Medicine, 2021-05-20;0(0):. 2021-05-20 [PMID: 34017133]

Mizuta K, Katou Y, Nakakita B et al. Ex vivo reconstitution of fetal oocyte development in humans and cynomolgus monkeys The EMBO journal 2022-08-01 [PMID: 35912849]

S Halin Berg, M Lundholm, A Nordstrand, A Bergh Rat prostate tumors induce DNA synthesis in remote organs Scientific Reports, 2022-05-12;12(1):7908. 2022-05-12 [PMID: 35551231]

Sebastiaan N Knoppert, Mandy G Keijzer-Veen, Floris A Valentijn, Marry M van den Heuvel-Eibrink, Marc R Lilien, Gerrit van den Berg, Lianne M Haveman, Marijn F Stokman, Geert O Janssens, Sven van Kempen, Roel Broekhuizen, Roel Goldschmeding, Tri Q Nguyen Cellular senescence in kidney biopsies is associated with tubular dysfunction and predicts CKD progression in childhood cancer patients with karyomegalic interstitial nephropathy. The Journal of pathology 2023-11-13 [PMID: 37792603]

More publications at http://www.novusbio.com/NB100-2280

Novus Biologicals USA
10730 E. Briarwood Avenue
Centennial, CO 80112
USA
Phone: 303.730.1950
Toll Free: 1.888.506.6887
Fax: 303.730.1966
nb-customerservice@bio-techne.com

Bio-Techne Canada
21 Canmotor Ave
Toronto, ON M8Z 4E6
Canada
Phone: 905.827.6400
Toll Free: 855.668.8722
Fax: 905.827.6402
canada.inquires@bio-techne.com

Bio-Techne Ltd
19 Barton Lane
Abingdon Science Park
Abingdon, OX14 3NB, United Kingdom
Phone: (44) (0) 1235 529449
Free Phone: 0800 37 34 15
Fax: (44) (0) 1235 533420
info.EMEA@bio-techne.com

General Contact Information
www.novusbio.com
Technical Support: nb-technical@bio-techne.com
Orders: nb-customerservice@bio-techne.com
General: novus@novusbio.com

Products Related to NB100-2280

NBL1-11424	Histone H2AX Overexpression Lysate
HAF008	Goat anti-Rabbit IgG Secondary Antibody [HRP]
NB7160	Goat anti-Rabbit IgG (H+L) Secondary Antibody [HRP]
NBP2-24891	Rabbit IgG Isotype Control

Limitations

This product is for research use only and is not approved for use in humans or in clinical diagnosis. Primary Antibodies are guaranteed for 1 year from date of receipt.

For more information on our 100% guarantee, please visit www.novusbio.com/guarantee

Earn gift cards/discounts by submitting a review: www.novusbio.com/reviews/submit/NB100-2280

Earn gift cards/discounts by submitting a publication using this product: www.novusbio.com/publications